acta physica slovaca vol. 53 No. 4, 267 – 278 August 2003

ON OPTICAL, ELECTRICAL AND STRUCTURAL PROPERTIES OF AMORPHOUS SILICON BASED SEMICONDUCTORS*

E. Pinčík[a 1], H. Kobayashi[b], J. Müllerová[c], K. Gmucová[a], M. Jergel[d], R. Brunner[a], M. Zeman[e], M. Zahoran[f]

[a] *Institute of Physics, Slovak Academy of Sciences, Dúbravská cesta 9, 842 28 Bratislava, Slovakia*

[b] *Institute of Scientific and Industrial Research, Osaka University, 8-1 Mihogaoka, Ibaraki, Osaka 5670047, Japan*

[c] *Department of Physics, Faculty of Logistic, Military Academy, SK–031 01 Liptovský Mikuláš, Slovakia*

[d] *Departmento de Física, CINVESTAV-IPN, Apdo. Postal 14-740, 07300 México D.F., México*

[e] *Delft University of Technology, DIMES, P.O. Box 5053, 2600 GB Delft, The Netherlands*

[f] *Faculty of Mathematics, Physics and Informatics, Comenius University, Bratislava, Slovakia*

Received 4 December 2002 in final form 25 April 2003, accepted 28 April 2003

The paper deals with structural and electrical properties of original, ion beam, and plasma exposed hydrogenated amorphous silicon (a-Si:H) surface. The a-Si:H semiconductor forms the intrinsic layer in amorphous silicon solar cells whose performance depends on the defect distribution, particularly on the density of dangling bonds. Device-quality intrinsic a-Si:H layer of approx. 1 μm thickness was deposited on n-type Si(100) oriented crystals in 13,56 MHz rf excited parallel plate plasma enhanced chemical vapor deposition system. Two types of surface exposures were made: by oxygen and argon plasmas. The Ar plasma-damaged surfaces were covered by an oxide layer prepared by *in-situ* exposure to pure oxygen atmosphere. In all cases, an uppermost very thin oxide overlayer of 5–10 nm thickness was formed, thicker than the native oxide formed after the PECVD of the amorphous layer. The optical and structural properties of original and damaged surfaces were investigated by reflectance spectroscopy and X-ray diffraction at grazing incidence, respectively. An important transformation of structural properties of aSi:H on Si(100) was investigated via the evolution of diffraction pattern around $2\Theta = 28.5^\circ$. Electrical properties were determined by the charge version of deep level transient spectroscopy, C-V and I-V measurements. Bias annealing procedures lead to the a MIS structure without deep states at the interface. The results obtained are compared with these measured on ion beam exposed a-Si:H surfaces [V. Nádaždy, R. Durný, E. Pinčík, Phys. Rev. Letters **78**; 1102 (1997)].

PACS: 73.20.At, 84.60.Jt, 79.60.Jv, 52.75.Rx, 07.07.Df

*Presented at Workshop on Solid State Surfaces and Interfaces III,Smolenice, Slovakia, November 19 – 21, 2002.
[1]The corresponding author

0323-0465/03 © Institute of Physics, SAS, Bratislava, Slovakia

1 Introduction

Both thin film solar cells and thin film transistors (TFT) usually contain amorphous silicon layers made by plasma enhanced chemical vapor deposition (PECVD). This type of the CVD has also the advantage that large-area devices can be manufactured from low-cost solar cells on glass, metal foil or polymer foil. During last years the additional study is focused on the properties of pin solar cells based on new low-cost material: polymorphous silicon. This material consists of an amorphous silicom matrix in which silicon particles are embedded [1]. In order to obtain higher conversion efficiences, while keeping the manufacturing cost low, a new development is introduced in low bandgap semiconductors in the multijunction device structure. The most common device is a p-i-n structure. A stabilized efficiency of light conversion in the corresponding solar cells depends on optical, electronic and structural properties, intrinsic a-Si:H layers used, its interfaces with p- and n-layers, and temporal and irradiation stabilities. The dominant transport mechanism of charge is drift. The built-in voltage between the highly doped p- and n-layers is distributed non-uniformly over the intrinsic layer. As the density of states is distributed over the band gap with increasing concentrations toward the valence and the conduction edges, the regions near the p- and n- layers contain a relatively high space charge density compared to the middle part of the intrinsic layer. If the intrinsic layer is made too thick or with too high density of states, the middle part of intrinsic layer becomes field-free and the charge transport is limited by diffusion. The presence of field-free regions can drastically reduce the collection efficiency.

Due to the presence of weak Si-Si bonds (strained bonds) and the relative ease of diffusive motion of hydrogen (movement of hydrogen atoms, molecules or ions at low temperatures through the defect sites in a-Si:H structure in comparison with movement in bulk c-Si), metastable dangling bonds can be created by breaking these weak bonds in addition to the initially present dangling bond density. This effect is known as the Staebler-Wronski effect [2]. The creation of metastable defects is driven by the release of energy due to electron-hole recombination events, and thus enhanced by an illumination of the material [2]. The increased dangling bond density reduces the electric field within the intrinsic part of the diode and enhances the recombination losses in the cell which deteriorates the cell performance. If p-i-n cell is made thin (less than 250 nm), it is not observed significant deterioration induced by the effect. Most probably, the drift-assisted charge-carrier collection length is not decreased to the values below the cell thickness, even though metastable dangling bonds are still created during the first houndred hours of exposure to solar irradiation (the diffusion length of the charge in a-Si:H is in the range of 100-200 nm). The Staebler-Wronski effect is self-limiting in time (or more precisely: it has an exponential decay with time). The conversion efficiency of a single-junction solar cells is thus stabilized at a value that is by about 20-30 % lower than the initial efficiency.

During last years, we have developed both technique and experimental equipment for the investigation of density of states in the amorphous silicon based semiconductors. The former is based on an original way to form device-quality very thin insulating layer (VTIL) in the surface region of amorphous semiconductors utilizing low-energy ion beam [3]. The latter is represented by a new charge deep level transient equipment (Q-DLTS) enabling us also the measurements of solid state voltcoulometry on thin film a-Si:H structures [4]. A very thin dielectric overlayer is needed for the realization of different operations and measurements on semiconductor films under higher voltages without a damage introduced by the deposition technique.

It was shown that gap states g(E) in amorphous silicon can be investigated by deep level tran-

sient spectroscopy (DLTS). Lang et al [5] and Cohen et al [6] presented a relationship between the density of gap states and DLTS spectra. The form of DLTS data is very close to the shape of g(E). There is a lack of new experimental results obtained on amorphous hydrogenated silicon (a-Si:H) using DLTS technique or dealing with the gap states on the basis of electrical methods - see review paper in [4].

For the interpretation of our results obtained by Q-DLTS, the defect-pool model of Winer [7] and Powell and Deane [8, 9] was used. It includes three basic group of states (0.63eV-D_h, 0.82 eV-D_z and 1.25 eV-D_e) which were identified by our charge version of DLTS [10, 11]. Our experiments indicate that the model of Powell and Dean is the most reliable one amongst others for a-Si:H semiconductor.

Semiconductor gap states are closely related to the structural properties, especially to the density of dangling bonds formed after the interaction of a structure with the energetic ions. As the most topical problem, the investigation of medium range order and formation of microcrystallities in a-Si:H semiconductor [12] can be mentioned.

The wavelength dependent refractive index, extinction coefficient, as well as the thickness of the film can be found by various spectrophotometric techniques and spectral IR ellipsometry. When the film is deposited on a transparent substrate, a so–called envelope method used for transparent films with the interference effects in transmittance and reflectance spectra is available. However, when the film is deposited on a thick absorbing substrate, only spectral reflectance measurements are possible. The optimised envelope method is suitable to obtain optical parameters of thin films on absorbing substrates simultaneously. The algorithm assuming a thin isotropic film with parallel interfaces is described here. It is applied for the determination of the optical parameters of a-Si:H thin films deposited by PECVD on c-Si(100) substrates.

In this paper, we focus our attention on the oxygen plasma treatment which should lead to the formation of the VTIL. The process of the interaction is evaluated mainly from from the point of view of evolution and important changes of electronic, structural and optical properties of the a-Si:H treated thin film. The main method to have been used is the reflectance spectroscopy providing the determination of optical parameters. In addition, we will also discuss the changes induced in the gap-state distribution and structural properties caused by the interaction of the original a-Si:H surface with low-energy ions coming from different sources (rf plasma and ion beam).

In the paper, we try to find the way how to suppress the interface states in the plasma treated a-Si:H structures. We will perform an original type of I-V meauserments which should give an evidence of hydrogen drift in $\sim 1\mu$m thick hydrogenated amorphous silicon. The VTILs of a high resistivity to the electrical breakdown can be prepared by both mentioned technologies and therefore they seem to be a promising techniques in future.

2 Spectral reflectance - description of theoretical approach

Optical characterisation of thin films gives information about other physical properties, e.g. band gap energy and band structure, optically active defects etc. which may be of permanent interest for several different applications. Considerable differences between optical constants of bulk material and thin films or those of films prepared under various growth conditions are often reported. This effect is significant for the multicomponent thin films prepared from bulk material

by e-beam evaporation. It leads to the changes of stoichiometry, structure, strain, etc. of material in thin film [13]. Optical measurements are carried out mostly by spectrophotometry or spectroscopic ellipsometry. The difference between various optical techniques is in the choice of at least two measurements of reflected or transmitted light and in the way of the inversion of reflection or transmission data to obtain optical constants values [14, 15, 16].

2.1 Interference reflection spectrophotometry

The refractive index, extinction coefficient, as well as the thickness of the film can be found from a transmittance $T(\lambda)$ or a reflectance $R(\lambda)$ spectrum of the film deposited on a transparent substrate. When the film is deposited on a thick absorbing substrate, only spectral reflectance measurement is possible.

A thin isotropic film with the average thickness d is characterised by the complex refractive index $n_1 = (n_1 - i\,k_1)$ and the substrate (with the thickness $>> d$) by the complex refractive index $n_2 = (n_2 - i\,k_2)$ where n_1 (n_2) is the complex refractive index and k_1 (k_2) is the extinction coefficient. The optical reflectance of a planparallel thin isotropic homogeneous film on a thick partly absorbing substrate, both immersed in air, is given as [14]:

$$R = \frac{A + Bx + Cx^2}{D + Ex + Fx^2} \tag{1}$$

where $x = \exp(-\alpha d)$ is the absorbance, $\alpha = (4\pi k_1)/\lambda$is the absorption coefficient, $\Phi = (4\pi n_1 d)/\lambda$, and

$$\begin{aligned}
A &= \left[(1-n_1)^2 + k_1^2\right]\left[(n_1+n_2)^2 + (k_1+k_2)^2\right], \\
C &= \left[(1+n_1)^2 + k_1^2\right]\left[(n_1-n_2)^2 + (k_1-k_2)^2\right], \\
D &= \left[(1+n_1)^2 + k_1^2\right]\left[(n_1+n_2)^2 + (k_1+k_2)^2\right], \\
F &= \left[(1-n_1)^2 + k_1^2\right]\left[(n_1-n_2)^2 + (k_1-k_2)^2\right], \\
B &= 2\left[A'\cos\Phi + B'\sin\Phi\right],\ E = 2\left[C'\cos\Phi + D'\sin\Phi\right], \\
A' &= \left(1-n_1^2-k_1^2\right)\left(n_1^2-n_2^2+k_1^2-k_2^2\right) + 4k_1\left(n_1k_2-n_2k_1\right), \\
B' &= \left(1-n_1^2-k_1^2\right)\left(n_1k_2-n_2k_1\right) - 2k_1\left(n_1^2-n_2^2+k_1^2-k_2^2\right), \\
C' &= \left(1-n_1^2-k_1^2\right)\left(n_1^2-n_2^2+k_1^2-k_2^2\right) - 4k_1\left(n_1k_2-n_2k_1\right), \\
D' &= \left(1-n_1^2-k_1^2\right)\left(n_1k_2-n_2k_1\right) + 2k_1\left(n_1^2-n_2^2+k_1^2-k_2^2\right).
\end{aligned} \tag{2}$$

where A', B', C', and D' are computational parameters for B and E without direct physical interpretation.

Since the equation is not reversible, a fitting procedure is necessary to calculate $n_1, k_1, d$and to get the best fit between the measured reflectance R_{exp} and the calculated value R. According to Eqs. (1), (2), the calculated reflectance $R(\lambda_1, n_1, k_1, d)$ is the function of three parameters n_1, k_1, d and can be fitted to the measured reflectance $R_{\text{exp}}$by several approaches such as e.g. by the least-square method and looking for global minimum or local minima for each parameter.

2.2 Envelope method

In the interference, especially in the transmittance spectrophotometry, the envelope method is often used [14, 15]. Obviously, only one independent parameter can be determined from a single reflectance measurement. When the film is slightly absorbing, interference effects coming from multiple coherent reflections at the interfaces are present in the reflectance spectrum and the above parameters can be determined from the envelopes $R_{\max}$ and $R_{\min}$ of the interference maxima and minima. A widely used version of envelope method has been developed by Swanepoel [14] for transmittance measurement. The versions based on the reflectance alone are seldom [16].

The reflectance R for the envelopes of the interference fringes can be expressed using the conditions for the interference maxima $2n_1d = m\lambda$ and the interference minima $2n_1d = (2m+1)\,\lambda/2, \quad |m| = 0,\, 1,\, 2\ldots$ Hence, the envelopes of the interference maxima $R_{\max}$ and interference minima $R_{\min}$ are given by Eq. (1) with the parameters A, C, D, F according to Eq. (2) but with the following parameters (for $n_1 < n_2$) for R_{max}:

$$\begin{aligned} B &= 2\left[\left(1-n_1^2-k_1^2\right)\left(n_1^2-n_2^2+k_1^2-k_2^2\right)+4k_1\left(n_1k_2-n_2k_1\right)\right]\,, \\ E &= 2\left[\left(1-n_1^2-k_1^2\right)\left(n_1^2-n_2^2+k_1^2-k_2^2\right)-4k_1\left(n_1k_2-n_2k_1\right)\right] \end{aligned}$$

and for $R_{\min}$:

$$\begin{aligned} B &= 2\left[\left(1-n_1^2-k_1^2\right)\left(n_1^2-n_2^2+k_1^2-k_2^2\right)+4k_1\left(n_1k_2-n_2k_1\right)\right]\,, \\ E &= -2\left[\left(1-n_1^2-k_1^2\right)\left(n_1^2-n_2^2+k_1^2-k_2^2\right)-4k_1\left(n_1k_2-n_2k_1\right)\right]. \end{aligned} \tag{3}$$

The equations for $R_{\max}, R_{\min}$ are non–linear equations of n_1, k_1. Expressing x from $R_{\max}$, $R_{\min}$ and equating them, a polynomial for the independent parameters n_1, k_1 is obtained at each wavelength. The optical parameters $n_1,\ k_1$ are determined numerically in several steps.

In the reflectance spectrum with the interference fringes, the assumption $n_1^2 >> k_1^2$ is valid. Assuming this in the polynomial obtained from $R_{\max}$, $R_{\min}$, we numerically solve n_1 and the initial value of k_1. Assuming $R_{\max}$, $R_{\min}$ to be continuous functions of the wavelength, $n_1,\ k_1$ as the functions of λ can be obtained. The initial value of k_1 is used in the recalculation of $n_1,\ k_1$ according to the above desribed procedure without the assumption $n_1^2 >> k_1^2$. The procedure of successive iterations should be repeated until the satisfactory accuracy in $n_1,\ k_1$is obtained.

Knowing n_1 as the function of λ, we calculate the thickness d according to the standard equation for two adjacent interference fringes at the wavelengths λ_m, λ_n: $d = \frac{\lambda_m\lambda_n}{2(\lambda_m n_n - \lambda_n n_m)}$ where n_m, n_n are refractive indices corresponding to these wavelengths. The average value of d is taken to find the order number of interference fringes. With the order numbers deduced, one recalculates the film thickness with the same $\mathrm{n}_1$as before. The improved thickness is used to perform the procedure again and to improve n_1 and k_1. With improved values of k_1 and d, the absorption coefficient α can be calculated.

The method suffers from multiple solutions $n_1,\ k_1$ of the polynomial. However, the identification of the correct solution without any other independent measurement is possible. A general procedure how to find the correct solution is to adjust the thickness and the optical parameters

to acceptable results of the dispersion dependence and to use some constraints restricting the number of degrees of freedom which requires, however, some previous physically meaningful knowledge of the material.

3 Sample preparation

Device-quality intrinsic a-Si:H layers of the thickness of $\sim$ 0.9 μm were deposited on the n-type Si(100) oriented crystals (phosphorus doped of 1-10 Ωcm conductivity) in a 13.56 MHz rf excited parallel plate plasma enhanced chemical vapor deposition system from pure SiH_4 and its mixture with H_2 at the plasma power of $\sim$ 40 W in the sample temperature of 195 $^\circ$C.

In the surface region of both types of amorphous silicon based thin films, ultrathin insulating overlayers were formed by following procedures:

i) Argon plasma treatment in a commercial RF plasma capacitively coupled equipment SECON XPL-200P was used. The frequency and power of the rf generator were 100 kHz and 60 W, respectively. The temperatures of the samples were kept in the 20 - 30 $^\circ$C range. A set of three samples was prepared at the working pressures 200 μbar, 500 μbar and 900 μbar of high purity Ar. Typical gas flow is approximately 100 sccm per minute. Special attention was paid to the first one which has the best resistivity. From the volt-ampere characteristics measured by cylindrical single probe localized in the central part of the plasma at 500 μbar, the following values of the plasma potential, ion density, electron temperature and ion flow density were determined, respectively: 45 V, 5x10^{14} m^{-3}, 3.0 eV and 1x10^{17} m^{-2} s^{-1}. At the calculation we assumed: a) the plasma is infinite, homogeneous and quasineutral in the absence of the probe; b) electrons and ions have Maxwellian velocity distributions with temperatures T_e and T_+ respectively, with $T_e >> T_+$; c) the mean free path of electrons and ions are large compared to all the other characteristic lengths; d) each charged particle hitting the probe is absorbed and is not reacting with the probe material; e) the region in the front of the probe surface, where the plasma parameters deviate from their values in the indistubed plasma is confined to a space charge sheat with a well defined boundary, outside of this boundary the space potencial is assumed to be constant; f) the sheat thickness is small compared to lateral dimensions of the plane probe (hence edge effect may be neglected). The argon treated surface was covered by very thin oxide layer prepared by "in situ" exposure of the surface to neutral high pure oxygen atmosphere.

ii) Oxygen plasma treatment in the same apparatus and under the same conditions as it is described in previous point excepting the oxygen working pressure. It was stabilized at 500 μbar, only.

iii) Ion beam treatment was made in two steps at the sample temperature of 80 $^\circ$C. First, the treatment by 350 eV argon positively charged particles with the dose of $\sim 10^{16}$ per cm^2. Second, the covering of the exposed surface by an insulator was performed by a low-energy ion beam composed of oxygen and hydrogen only, with the dose of $\sim$ 2x10^{15} per cm^2. For the low energy ion beam exposure of the surface we have used commercial ion beam etching system of LPAI Comp. with Kauffman plasma source. This type of samples serves as the reference for those prepared by plasma treatment. The older results obtained on similar structures were published e.g. in [4].

4 Experiment, results, and discussion

4.1 Reflectance spectroscopy

Reflectance measurements were carried out by a double–beam Carl Zeiss Jena spectrophotometer Specord M40 with the slit of 2.5 nm at room temperature. An accessory for absolute reflectance measurement at nearly normal incidence was used with a freshly evaporated aluminium sample in the reference beam and special care was taken to ensure the reproducibility of measurements. The values of n_2, k_2 were taken from [17] and confirmed by the Kramers–Kronig dispersion analysis of Si substrate reflectance spectrum. No significant differences were found between the reflection spectra from different areas of the samples. As the probed area was $\sim 0.2cm^2$, the films can be considered homogeneous at least down to this scale.

Reflectance spectra were recorded on the reference and oxygen plasma exposed samples. The optical constants of the samples under study retrieved by the envelope method are shown in the figures in the following order.

Fig.1 and Fig.2: Dispersions of refractive index and extinction coefficient (the reference and plasma treated samples, respectively);

Fig.3 and Fig.4: Dispersions of absorption coefficient;

Fig.5 and Fig.6: Determination of Tauc bandgap width for both types of samples.

The reference samples have lower real part of refractive index in comparison with tabelled values (see [18]). It means that stoichiometry of the a-Si:H layer was disturbed at the begin of the experiment. We supposed that the layers were more porous. The exposure to oxygen plasma lowered the refractive index. This result and electrical DLTS measurements indicate that part of hydrogen was removed and substituted by oxygen also in thin film volume. The shape of the reflectance spectra as well as the results of their theoretical analyses confirmed that the some optical properties of the amorphous silicon layer were considerably changed. It is evidenced that important changes concern of the complex refractive index and absorption coefficient. On the other side, we cannot explain why the Tauc bandgap widths E_g of the reference and oxygen plasma treated samples are the same (∼1.78 eV). It means that the most important optical property of aSi:H semiconductor was not modified. The next set of investigated samples have been made by exposure to argon plasma followed "in situ" by oxidation of the disturbed surface by neutral oxygen gas - see point i) of part 3 (Sample preparation). This is the experiment similar to that in which monoenergetical argon atoms of low energy were used for the preparation of the device quality VTIL [10].

4.2 Charge version of deep level transient spectroscopy (Q-DLTS), capacitance-voltage (C-V) and current-voltage (I-V) dependences

The modified charge-based correlation DLTS method [19] was used to study the metal (gold)-oxide-amorphous semiconductor (MOS) structures. This method is based on the correlation approach, i. e. the transient response of the MOS structure under periodically applied voltage steps to the gate electrode is measured, and subsequently a weighted combination of the charge signals obtained at various sampling events is achieved. The sampling events, as well as the weighting coefficients used in our work, are chosen with the aim to improve the selectivity in the measured spectrum. The resulting correlated charge DLTS signal S_c is described by a weighted

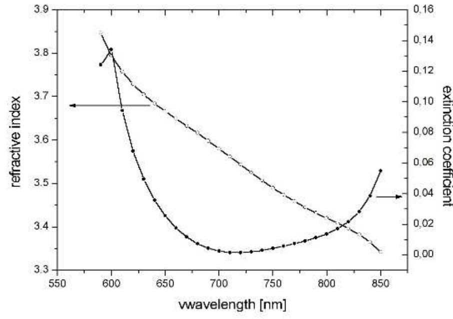

Fig. 1. Dispersions of refractive index and extinction coefficient of the reference (as prepared) a-Si:H layer deposited on c-Si substrate.

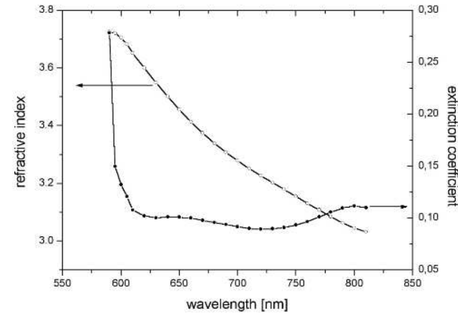

Fig. 2. Dispersions of refractive index and extinction coefficient of oxygen exposed a-Si:H layer deposited on c-Si substrate

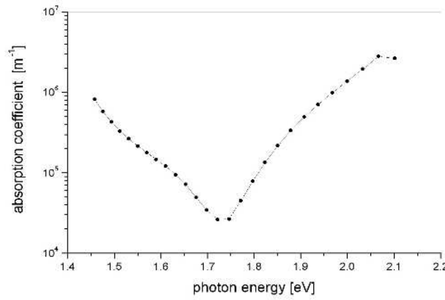

Fig. 3. Dispersion of absorption coefficient of the reference layer

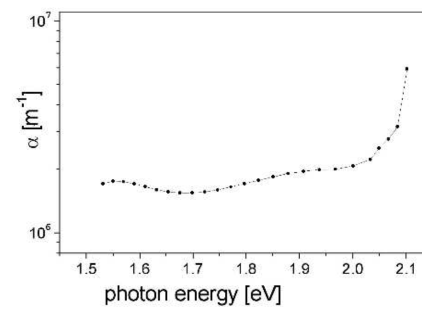

Fig. 4. Dispersion of absorption coefficient of the oxygen plasma exposed layer.

summation of the contributions from three channels. The parasitic output charge due to the presence of a leakage current is eliminated by the used filtering scheme. The following formula is valid for the measured Q-DLTS signal comming from a deep trap:

$$\Delta Q \approx \left[\frac{C_{ox}}{C_{ox} + C_s}\right] q \cdot w \cdot N_T \cdot \exp\left(-e_n\, t\right) \tag{4}$$

where w stands for the excited part of the depletion region, N_T for the trap density, C_{ox} and C_s for both the capacitance of the oxide and the capacitance of the space charge layer, respectively. The emission rate from the trap at the energy ΔE above the conductance band is

$$e_n = v \cdot \sigma_n \cdot N_c \cdot \exp\left(-\frac{\Delta E}{kT}\right) \tag{5}$$

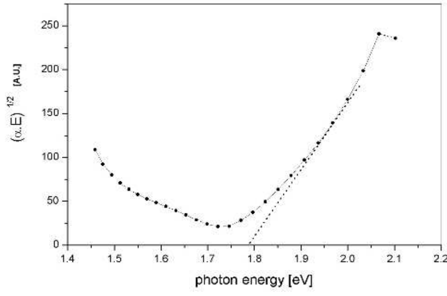

Fig. 5. Determination of Tauc band gap width for the reference layer

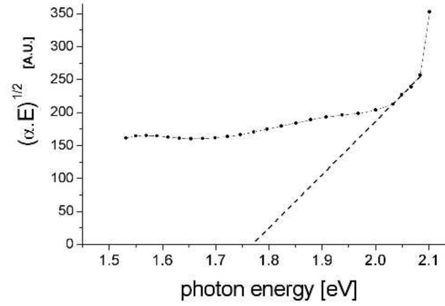

Fig. 6. Determination of Tauc band gap width for the oxygen plasma exposed layer.

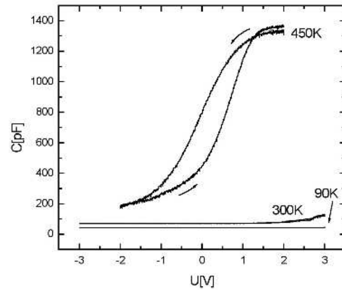

Fig. 7. C-V curves of sample prepared at 200 μbar by argon plasma exposure.

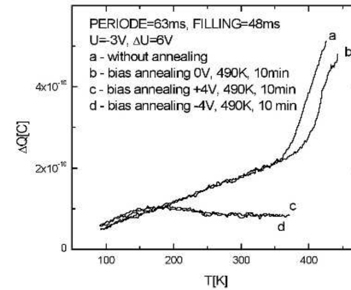

Fig. 8. Q–DLTS measurements of the 200 μbar sample.

where ν is the mean thermal velocity of electrons, σ_n is the capture cross section and the N_c is the effective density of states in the conduction band. The DLTS response of the above mentioned structure was measured at sampling events chosen to fit the following scheme: t_1, $2t_1$ and $4t_1$. The resulting correlated charge DLTS signal S_c can be described as

$$S_c = Q\,(t_1) - 1.5\,Q\,(2\,t_1) + 0.5\,Q\,(4\,t_1) \qquad (6)$$

The experimental results obtained by C–V, Q–DLTS and I–V methods on the samples prepared by plasma exposure at the argon pressure of 200 μbar are shown in Figs.7-9, respectively.

The structure prepared by argon ion beams contains three basic groups of states, namely 0.63eV-D$_h$, 0.82 eV-D$_z$ and 1.25 eV-D$_e$ as it was published in [20]. We can state that :

i) High resistive VTILs with the capacitance of $\sim$ 1 500 pF were prepared (Fig.7). The results are similar to those of the experiments with a low energy argon ion beam exposure - see e.g. [10].

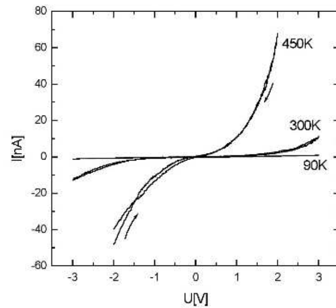

Fig. 9. I-V dependence of the 200 μbar sample.

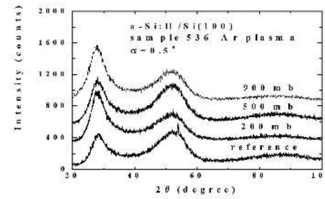

Fig. 10. XRDGI patterns of plasma exposed samples scanned at incidence angle 0.5 $^\circ$.

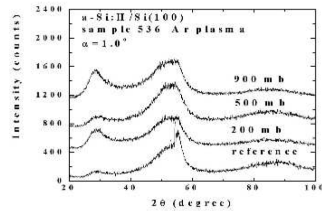

Fig. 11. XRDGI patterns of plasma exposed samples scanned at incidence angle 1 $^\circ$.

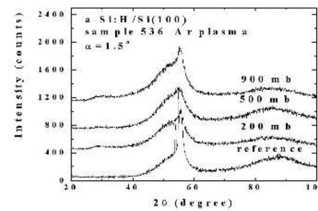

Fig. 12. XRDGI patterns of plasma exposed samples scanned at incidence angle 1.5 $^\circ$.

ii) The deep level spectra contain only the high temperature tail, which can be suppressed by bias annealing procedure (see Fig. 8). We suppose that the observed tail is caused not only by the increased electrical conductivity of the system (as a consequence of thermal heating), but also by a rest of D_z states.

iii) I-V measurements did not confirm a motion of hydrogen ion, because no voltammetric wave is present at negative biasing [21]. A plot of the respective measurement is shown in Fig.9.

The electrical measurements are in agreement with the optical ones because they confirmed that a-Si:H layers have lost their typical character given by the hydrogen content. We suppose that the hydrogen content in the layer was considerably decreased. After the interaction, a polycrystalline Si state characterized by both reduced density of hydrogen related bonds and its mixture with oxygen begins to dominate.

4.3 X-ray diffraction at grazing incidence (XRDGI)

The XRDGI was measured on the 12 kW Rigaku rotating-anode generator with the CuK_α radiation using a wide-angle position sensitive Inel detector. The diffractometer was equipped with a graphite monochromator in the primary beam.

The XRDGI patterns taken from the whole pressure set of the samples prepared by plasma treatment at 0.5°, 1.0° and 1.5° incidence angles are shown in Figs.10-12.

The samples with crystalline silicon (100) substrate were measured. The dominant signal comes from the amorphized (100) cubic surface, namely 311 and 422 diffractions. An additional signal observed at $\sim 28^\circ$ is typical for the a-Si:H layer. Its intensity decreases with increasing incidence angle, i.e. with the increasing depth the diffracted X-rays come from. This maximum could be identified (using the PDF 2 database [22]) as the diffraction originating from the multiatomic Si-H groups such as $Si_{80}H_{20}$complexes.

We can state that all plasma exposed samples have an increased density of $Si_{80}H_{20}$ complexes (see the development of the angular region around $2\Theta = 28^\circ$). This result is in accord with the results of both optical and electrical measurements and confirms a drastic decrease of hydrogen content in the a-Si:H thin films after the argon plasma treatment.

5 Conclusion

The wavelength-dependent refractive index, extinction coefficient, and the thickness of thin films were retrieved from the reflectance spectra. It was shown that the electrical, optical and structural properties of original a-Si:H 1 μm thin film deposited on c-Si(100) were considerably transformed after the interaction with the low temperature rf oxygen and argon plasmas of short duration. The following conclusions can be done :

i) The reference samples have lower real part of refractive index in comparison with tabelled values. We suppose that the stoichiometry of the a-Si:H layer was disturbed at the begin of the experiment and that the layers were more porous as the standard device quality layers. The exposure to oxygen plasma additionally lowered the refractive index. This result and electrical DLTS measurements indicate that part of hydrogen was removed and substituted by oxygen also in thin film volume.

ii) The high resistive VTILs were prepared in the surface region of a-Si:H at the argon pressure of 200 μbar. The result is similar to the experiments with a low energy argon ion beam exposure. The interface properties (from the point of view of density of states) are improved (see below).

iii) The deep level spectra contain only the high temperature tail, which can be fully suppressed by a bias annealing procedure. It means, that we have prepared the sample with considerably suppressed density of deep states at the measured interface. We suppose that the observed tail is a rest of D_z states.

iv) A drift of hydrogen ions in the structures was not observed.

v) Plasma exposed samples demonstrate that an increased part of the volume is occupied by $Si_{80}H_{20}$ complexes as judged from the increased intensity of the corresponding diffraction peak.

Acknowledgement: This work was partly supported by the Slovak Grant Agency (VEGA), projects No: 2/1119/22, 2/1013/22 and by Slovak Powerplants, Inc.

References

[1] P. Roca i Cabarrocas, P. Sahel, S. Hamma, and Y. Poissant, In: Proceedings of 2nd Word Conference on Photovoltaic Solar Energy Conversion, Vienna, Austria, 6-10 July 1998, Vol. 1, p. 355, edited by J. Schmid et al., published by Joint Research Centre, European Commission.

[2] D.L. Staebler, C.R.Wronski, Appl. Phys. Lett. **31**, 292 (1977).

[3] R. Durný, E. Pinčík, V. Nádaždy, M. Jergel, J. Shimizu, M. Kumeda, T. Shimizu, Appl. Phys. Lett. **77**; 1783 (2000).

[4] I. Thurzo, V. Nádaždy, In: T. Searle (edit.): Amorphous Silicon and its Alloys, INSPEC, The Inst. of Electr. Engin., London, UK 1998, pp. 151-160.

[5] D.V. Lang, J.D. Cohen, J.P. Harbison, Phys. Rev. B **25**; 5285 (1982).

[6] J.D. Cohen, D.V. Lang, Phys. Rev. B **25**; 5321 (1982).

[7] K. Winer, Phys. Rev. B **41**; 12 150 (1990).

[8] M.J. Powell, S.C. Deane, Phys. Rev. B **48**; 10815 (1993).

[9] M.J. Powell, S.C. Deane, Phys. Rev. B **53**; 10121 (1996).

[10] V. Nádaždy, R. Durný, E. Pinčík, Phys. Rev. Letters **78**; 1102 (1997).

[11] V. Nádaždy, R. Durný, E. Pinčík, I. Thurzo, M. Kumeda, T. Shimizu, J. of Non-Cryst. Solids **266-269**; 558 (2000).

[12] S. Acco, D.L. Williamson, S. Roorda, W.G.J.N.M. van Sark, A. Polman, W.F. van der Weg, J. Non-Cryst. Solids **227-230**; 128 (1998).

[13] F. Kundracik, M. Hartmanová, J. Müllerová, M. Jergel, I. Kostič, R. Tucoulou, Mater. Sci. Eng. **B84**; 167 (2001).

[14] D. Minkov, R. Swanepoel: Optical Engineering, **32** (1993) 3333

[15] M. Nenkov, T. Pencheva: J. Opt. Soc. Am. **15** (1998) 1852

[16] J.M. Gonzalez-Leal, E. Marquez, A.M. Bernal-Oliva, J.J. Ruiz-Perez, R. Jimenez-Garay: Thin Solid Films **317** (1998) 223

[17] V.I. Gavrilenko, A.M. Grechov, D.V. Korbutjak, V.G. Litovchenko: Optical parameters of semiconductors, Naukovaja dumka, Kiev, 1978, in Russian

[18] Ed.: E.D. Palik, Handbook of Optical Constants of Solids, Academic Press, Inc., Orlando, 1985.

[19] K. Gmucová, I. Thurzo, E. Pinčík, Phys. Stat. Sol. a **135**; 315 (1993).

[20] E. Pinčík, M. Jergel, C. Falcony, L. Ortega, H. Glesková, J. Müllerová, R. Brunner, S. Mráz, K. Gmucová, Superficies y Vacio **13**; 34 (2001).

[21] I. Thurzo, K. Gmucová, J. Orlický, J. Pavlásek, Rev. Scient. Instr. **70**; 3723 (1999).

[22] File No. 41-788 of the Powder Diffraction Database (PDF 2) of JCPDS-ICDD diffraction data available from the International Centre for Diffraction Data, Newton Square, PA, www.icdd.com.